Low-frequency inelastic light scattering from chalcogenide glasses and alloys*

R. J. Nemanich†
Department of Physics, James Franck Institute, University of Chicago, Chicago, Illinois 60637
(Received 9 September 1976)

Polarized low-frequency Raman and Brillouin spectra of the chalcogenide glasses As_2S_3, GeS_2, $GeSe_2$, and As_2Se_3 and the glass alloy system $(As_2S_3)_{1-x}(GeS_2)_x$ have been measured using the near infrared 7525 or 7993 Å lines of a krypton laser. The low-temperature $T \sim 10$ K spectra of the four binary glasses indicate that the Raman coupling constant exhibits an ω^2 frequency dependence in the limit $\omega \rightarrow 0$. In addition it is demonstrated that the spectral distribution of the low-frequency low-temperature Raman coupling constant can be described by a model proposed by Martin and Brenig. By fitting the predicted spectra of the model to the experimentally obtained spectra, the structural correlation ranges of the glasses have been determined. It is found that the structural correlation ranges of the As_2S_3 and As_2Se_3 glasses are 6.5 ± 1 Å, while those of the GeS_2 and $GeSe_2$ glasses are 8.5 ± 1 Å. These results are compared with values of structural correlations obtained from x-ray diffraction spectra and optic-mode Raman spectra. The depolarization spectra predicted from the Martin and Brenig model are found to deviate significantly from the observed low-frequency depolarization spectra of the chalcogenide glasses. At higher temperatures the low-frequency Raman spectra of all samples exhibit a feature apparently centered at 0 frequency shift which cannot be described by the model of Martin and Brenig. A similar feature termed the light scattering excess has been reported for the low-frequency Raman spectrum of fused silica. A recent model by Theodorakopoulos and Jäckle describes the light scattering excess in terms of two-level defect states. The temperature dependence, depolarization ratio, and spectral distribution of the light-scattering excess are interpreted using this model and recent ultrasonic attenuation measurements. The composition dependence of both the structural correlation range and the light-scattering excess is presented for the alloy system of $(As_2S_3)_{1-x}(GeS_2)_x$.

I. INTRODUCTION

There has been a considerable contribution to the understanding of the structure of disordered solids from light-scattering investigations.[1] These studies have concentrated predominantly on spectral features which occur in the optic-mode region of the Raman spectra of disordered solids. Recently interest has developed in the spectral features in the low-frequency or acoustic region. Part of this interest is a manifestation of a thorough theoretical development of the properties of light scattering from Debye-like acoustic modes in disordered solids by Martin and Brenig.[2] This development described the features of the low-frequency Raman spectra in terms of the structural properties of the amorphous solids. Thus measurement of light scattering from long-wavelength acoustic modes of disordered solids may yield unique structural information. While there have been some experimental investigations of disordered solids that have focused on the light scattering from acoustic modes,[3-7] there has been, to our knowledge, no experimental verification of the Martin and Brenig theory as it applies to bulk glasses.

In addition to the light scattering at low-frequency shifts due to acoustic phonons, another spectral feature has recently been reported in the low-frequency Raman spectrum of fused silica and two other glasses.[8,9] This feature termed the "light-scattering excess" has been attributed to the same defect states that have been invoked[10,11] to describe the anomalous linear T-dependent term in the low-temperature specific heat of glasses.[12,13]

While both of the topics, light scattering from acoustic modes and the light-scattering excess, have been subjects of a limited number of recent investigations, they have been treated separately. Because both effects are observed at Raman shifts of less than 50 cm^{-1}, they are at least experimentally and perhaps theoretically intimately connected. The low-frequency Raman spectra of glasses reflects features of both processes.

In light of the previous work of Martin and Brenig it is important that the validity and/or limitations of their theory be determined and that the dependence of the light scattering from acoustic modes on the amorphous structure be studied. Also it is of interest to ascertain whether the light-scattering excess is a general property of bulk glasses and to determine if it too is dependent on structure.

In this paper the polarization and temperature dependence of the low-frequency Raman spectra of several chalcogenide glasses will be examined to determine not only the general properties of light scattering from acoustic modes and the light-scattering excess but also to ascertain structural

properties of the specific glasses. The glasses to be used in this investigation are As_2S_3, GeS_2, As_2Se_3, $GeSe_2$, and the mixed glass alloy system $(As_2S_3)_{1-x}(GeS_2)_x$. The chalcogenide glasses are ideal choices for this experiment for several reasons, not the least of which is that there has been considerable research to determine their amorphous structures.[14-16] All the solids to be studied here can be prepared as well-characterized high-optical-quality, bulk glasses. Good sample optical quality is important to minimize the spectral component due to parasitically scattered light which masks the low-frequency Raman spectra. In addition, the chalcogenide glasses can be easily alloyed,[16] therefore properties which arise from differences in structure can be studied in detail.

All of the chalcogenide glasses to be studied here have compositions which are characterized as chemically ordered.[16] Previous studies on chalcogenide glasses in the chemically ordered phase have indicated that like-atom bonds do not occur.[14-17] These studies have also indicated that the short range order of these glasses is characterized by specific local atomic clusters or structural units. For As_2S_3 and As_2Se_3 the cluster is an AB_3 pyramidal unit with the threefold coordinated As atom at the apex. For the glasses GeS_2 and $GeSe_2$ the cluster is an AB_4 tetrahedron with the fourfold coordinated Ge atom at the center. These local clusters are interconnected through the twofold coordinated chalcogenide atom. Also each member of the mixed glass alloy system $(As_2S_3)_{1-x}(GeS_2)_x$ is composed only of AsS_3 pyramidal units and GeS_4 tetrahedral units.[16]

It is well known now that the mechanisms for first-order Raman scattering from crystalline solids differs from that for scattering from amorphous materials.[1] The first-order vibrational Raman spectra of crystals are usually composed of sharp lines, and the Raman process is characterized by inelastic scattering which conserves both energy and crystal momentum.[18] The Raman spectra of amorphous materials are in general continuous with broad spectral features.[1] Shuker and Gammon have shown that a short structural correlation length leads to a breaking of the crystal momentum selection rules.[19] In glasses the assumption of a short correlation range is justified, and the continuous Raman spectra obtained are ascribed to disorder-induced scattering. From the theoretical investigation of Shuker and Gammon, the stokes Raman intensity was found to be

$$I_{\alpha\beta,\gamma\delta}(\omega)=\sum_b C^{(b)}_{\alpha\beta,\gamma\delta}(\omega)G_b(\omega)\left(\frac{n(\omega)+1}{\omega}\right), \qquad (1)$$

where $G_b(\omega)$ is the density of states, $n(\omega)$ is the boson thermal occupation number, and $C^{(b)}_{\alpha\beta,\gamma\delta}(\omega)$ is the Raman coupling constant or matrix element. The sum is over all bands, and $\alpha\beta, \gamma\delta$ are polarization indices.

The coupling constant (C) was originally postulated to be frequency independent over any particular band.[19] Thus the Raman spectra of disordered solids, when reduced by the harmonic-oscillator term $[n(\omega)+1]/\omega$, reflects the density of states modulated by the coupling constant. Reduced Raman spectra of amorphous Ge films represented with reasonable agreement the smoothed crystalline density of vibrational states in the optic-mode region.[20] Moreover, the spectrum of amorphous Ge films was polarization independent.[20] Therefore, it was suggested that C was both frequency and band independent in the optic-mode region.

In contrast, Raman spectra of bulk chalcogenide glasses are polarization dependent in the optic-mode region.[15-17] Also the strongest modes observed in infrared (ir) reflectivity measurements of these glasses were weak or not observable in the corresponding Raman spectra and vice versa.[16,17] Thus spectral features of the chalcogenide glasses were described theoretically in terms of the normal vibrations of the local atomic structural units,[14] and mode symmetries were verified by Raman polarization characteristics and ir or Raman activity.[16,17] From these results it had become evident that the Raman coupling constant in the optic-mode region was clearly band dependent, but still C is expected to vary weakly with frequency over any particular band.

Exact determination of the frequency dependence of the Raman coupling constant is in most cases impossible because there are few amorphous materials for which the density of states has been determined experimentally. But in the low-frequency region where the vibrational modes are acoustic the density of states may be expected to be Debye-like and thus exhibit an ω^2 dependence.[3] Neutron-diffraction measurements on a-Se indicate Debye ω^2 behavior up to $\sim 50\ cm^{-1}$.[21] Thus the range of Raman shifts $\omega < 50\ cm^{-1}$ becomes ideal for studying the frequency dependence of the Raman coupling constant. Also, in the low-frequency region sharp spectral features which arise from momentum conserving light scattering from the acoustic modes are observed.[22,23] Thus both momentum conserving and nonconserving scattering takes place in the low-frequency region.

Whalley and Bertie first considered light scattering from an electrically irregular medium.[24] In that study molecules were considered to be in regular positions of a crystal lattice, but rotationally disordered. They showed that momentum allowed Brillouin lines would be imposed on a

background due to disorder-induced scattering in which the magnitude of the Raman matrix element for each vibrational mode is proportional to ω^2. Prettl, Shevchik, and Cardona also obtained an ω^2 frequency dependence of the Raman coupling constant for acoustic modes.[3] This result was obtained by calculating the contribution to the Raman tensor for vibrations of a disordered one-dimensional chain in which the structural unit possesses inversion symmetry. And as mentioned previously Martin and Brenig have carried out a detailed calculation of light scattering from an optically thick amorphous film.[2] This calculation included not only electrical disorder but also mechanical disorder. The results of this work showed again that the Brillouin peaks would be superposed on a disorder-induced background, and it was also predicted that at very low frequencies the coupling constant would be proportional to ω^2 but would deviate from this frequency dependence as ω increases. The deviation was found to be dependent on the structural properties of the specific amorphous material and the velocities of transverse and longitudinal sound waves.

There have been several recent experimental efforts to determine the frequency dependence of the Raman coupling constant in the low-frequency region.[4,6,7] Lannin has shown that $C \propto \omega^2$ in the low-frequency Raman spectrum of amorphous Si films.[4] His experiment was conducted in the backscattering configuration, and thus a large contribution to the observed spectra due to elastically and parasitically scattered light had to be subtracted from the low-frequency Raman spectrum before analysis. Papatheodorou and Solin, and Gorman and Solin, have studied the low-frequency Raman spectra of the bulk glasses As_2O_3 and Se, respectively, in the 90° transmission Raman configuration.[6,7] Both of these experiments yield an approximately frequency-independent coupling constant in the range of Raman shifts of 15–30 cm^{-1}. Thus the frequency dependence of the Raman coupling constant for light scattering from acoustic modes has not been clearly experimentally determined.

Once the low-frequency Raman scattering from acoustic phonons can be described accurately, the light-scattering excess can be studied more quantitatively. The spectral feature which has been termed the "light-scattering excess" is manifested in the room-temperature, low-frequency Raman spectrum of fused silica as an approximately constant intensity as $\omega \to 0$ below ~ 10 cm^{-1}.[8,9] Winterling discussed this spectral feature in terms of relaxation effects of, or direct optical coupling to the structural defects in a glass.[8] Previously, phonon-assisted quantum-mechanical tunneling of defects in glasses has been used by Anderson, Halperin, and Varma[10] and independently by Phillips[11] to describe both the linear temperature contribution to the low-temperature specific heat and the more recently observed low-temperature dependence of the attentuation of ultrasonic modes. Jäckle has pointed out that thermal relaxation of the defects should cause a peak in the ultrasonic attentuation at higher temperatures.[25] This peak has been observed in fused silica.[26] In a recent study Theodorakopoulos and Jäckle have considered both quantum-mechanical tunneling and thermal relaxation of defect states as possible origins for the light-scattering excess.[27] They suggest that the light scattering excess observed in fused silica at temperatures above 40 K arises from thermally activated structural relaxation of the defects. They also predict that at $T < 10$ K light scattering from phonon-assisted quantum-mechanical tunneling may be observable in the low-frequency Raman spectra of glasses.

II. EXPERIMENTAL

All samples except As_2S_3 were obtained from Xerox Corp. The preparation technique is described elsewhere.[16,17] The As_2S_3 was obtained from Cervo Corp. The samples were parallelepipeds of approximately $6 \times 3 \times 2$ mm^3 and were optically polished on the four larger faces. The optical quality of all samples except As_2Se_3 was quantitatively determined as follows. The intensity of either 6328 or 7525 Å linearly polarized laser radiation transmitted through the sample stationed between crossed and parallel polarization analyzers was measured. The transmitted intensity of the two configurations differed by factors ranging from 22 to 38 dB depending on the sample. Thus all samples exhibited high optical quality.

The materials studied had optical band gaps varying from the near infrared to well into the visible. While $GeSe_2$ and all the $(As_2S_3)_{1-x}(GeS_2)_x$ alloys are transparent to 7525-Å radiation at room temperature, As_2Se_3 highly absorbs even 7993-Å radiation at room temperature. But for all samples the optical gap increases dramatically at low temperature, and at $T \leq 60$ K As_2Se_3 is transparent to 7993-Å radiation.

A CRL 52G krypton ion laser with cavity mirrors optimized in the near infrared was used to excite the Raman spectra. The 7525- and 7993-Å lines of the krypton laser which were used here are often overlooked as possible radiation sources for Raman spectroscopy. All Raman spectra were acquired in the 90° transmission configuration. The scattered light was collected with $f/1.8$ optics for both room-temperature and low-temperature

measurements. For sample temperature other than room temperature a five-window throttling-type Andonian Dewar was used. This Dewar provides sample temperature ranging from ~2 K (with the sample immersed in superfluid He) to greater than 300 K. The temperature was measured by a silicon resistor located in the copper sample holder.

A Jarrell-Ash model 25-100 double monochromator equipped with Jobin Yvon, 1800-g/mm, 0.5-μm "blaze" holographic gratings was used to disperse the scattered light. An RCA C31034 photomultiplier tube was used for detection. This photomultiplier which has a GaAs photocathode has a high quantum efficiency of ~7% in the near infrared region. An Ortec modular photon counting system was used for detection. The data was recorded in both analog and digital form using a strip-chart recorder and teletype with paper-tape output, respectively.

The most severe problem in obtaining low-frequency Raman spectra is that the wings from the parasitic and elastically scattered light often obscure the region of interest. Therefore it is important to use samples of high optical quality and to avoid scattering from surfaces. As mentioned previously all samples used were of high optical quality. In addition, the monochromator entrance slit was carefully apertured in such a way that scattered light arising from surfaces perpendicular to the incident laser beam would not enter the monochromator. Also a spectral slit width of between 0.8 and 1 cm^{-1} was necessary not only for high-resolution measurements but also to allow examination of the Raman spectrum to a Raman shift as low as 3 cm^{-1}. In fact by using our Raman spectroscopic apparatus at the limits of its resolving capacity (~0.08 cm^{-1}) we were able to obtain high-quality polarized room-temperature Brillouin spectra of most of the glasses for which Raman data was acquired.

To eliminate phototube saturation effects which may occur after a strong signal, Stokes and anti-Stokes Raman spectra were scanned from larger Raman shifts to 0. Also to avoid electronics time-constant effects and to obtain low statistical noise spectra the monochromator was scanned at a rate of between 1 and 3 cm^{-1} per min. A time constant of 5 or 10 sec was used in recording the analog data on a strip-chart recorder while the digital data was accumulated in 10-sec intervals and recorded with the teletype paper-tape drive unit.

The low-frequency Raman spectra had maximum signal intensities of from 50 to 1000 counts/sec depending on the temperature, polarization, and the particular sample. Signal intensity in the 5–10-cm^{-1} region was considerably less than the maximum, therefore the dark count rate was carefully determined to facilitate analysis. The electronic lower level discriminator was set to obtain a dark count rate of less than 1.5 counts/sec.

All spectra reported here were polarization analyzed using two distinct geometries, one with the incident beam polarized and scattered light analyzed perpendicular to the scattering plane ($\perp\perp$), and one with the incident beam polarized parallel to and the scattered light analyzed perpendicular to the scattering plane ($\parallel\perp$). In addition, the instrument transfer function was carefully measured using a standard blackbody radiation source. All digital Raman spectra presented in this paper are corrected not only for the instrument transfer function but also for the ν_0^4 (where ν_0 is the frequency of the Raman photon not the frequency shift) dependence of the scattered radiation.

The low-frequency Raman spectra of all the samples except As_2Se_3 were excited with between 50 and 70 mW of 7525-Å radiation focused on the sample. There was no sign of signal deterioration due to photodarkening effects, but the low-temperature spectra of As_2Se_3 recorded with 7993-Å radiation slightly defocused showed some slow loss of intensity in the optic-mode region that can be attributed to photodarkening.[28,29]

III. RESULTS AND DISCUSSION

A. Scattering from long-wavelength phonons

1. Aspects of the model

In order to put the experimental results of this investigation into proper perspective, the model for low-frequency light scattering proposed by Martin and Brenig (MB) will be briefly described.[2] As mentioned before the model includes effects due to both mechanical and electrical disorder. The electrical disorder is manifested in the spatial fluctuations of the photoelastic constants while the mechanical disorder is accounted for by the spatial fluctuations of the strain tensor. In the MB model all spatially fluctuating quantities were assumed to exhibit simple Gaussian correlations with the same characteristic correlation range; namely the structural correlation range (SCR). This conclusion is justified because all spatial fluctuations arise essentially from the mechanical disorder for the chemically ordered glasses used in this study.

For the experiments described here, the $I_{\perp\perp}$ and $I_{\parallel\perp}$ components correspond to the Raman intensities I_{yyyy} and I_{yzzy}, respectively. Thus for this case the pertinent results of the MB model are as follows:

$$I^{(\omega)}_{\alpha\beta\gamma\delta} \propto f(\omega)\{\mathcal{B}_{\beta\alpha\gamma\delta} + x^2[\, g_t(x)E^t_{\beta\alpha\gamma\delta} + g_l(x)E^l_{\beta\alpha\gamma\delta}]\}\ , \quad (2)$$

where

$$x = 2\pi c(\omega/v_l)\sigma\ , \quad (3a)$$

$$2\sigma = \mathrm{SCR}\ , \quad (3b)$$

$$f(\omega) = |\omega|\{n(\omega)\Theta(\omega) + [n(\omega)+1]\Theta(\omega)\}\ , \quad (3c)$$

$$g_l(x) = e^{-x^2}\ , \quad (3d)$$

$$g_t(x) = (v_l/v_t)^5 \exp[-x^2(v_l/v_t)^2]\ , \quad (3e)$$

$$E^t_{yyyy} \simeq \tfrac{2}{15} C_t^2(\delta C_t^2/C_t^2 + \lambda)\ , \quad (3f)$$

$$E^l_{yyyy} \simeq C_l^2(\delta C_l^2/C_l^2 + \lambda) + \tfrac{4}{45} C_t^2(\delta C_t^2/C_t^2 + \lambda)\ , \quad (3g)$$

$$E^t_{yzzy} \simeq \tfrac{1}{10} C_t^2(\delta C_t^2/C_t^2 + \lambda)\ , \quad (3h)$$

$$E^l_{yzzy} \simeq \tfrac{1}{15} C_t^2(\delta C_t^2/C_t^2 + \lambda)\ , \quad (3i)$$

$$C_l/C_t = \tfrac{1}{3}(p_{11} + 2p_{12})/(p_{11} - p_{12})\ . \quad (3j)$$

Here ω is the frequency shift in cm^{-1}, v_l is the longitudinal velocity of sound, v_t is the transverse velocity of sound, $\Theta(\omega)$ is the usual step function, and p_{ij} are the elasto-optic constants. The term $\mathcal{B}_{\beta\alpha\gamma\delta}$ contains the terms that describe the momentum-conserving Brillouin peaks, and $n(\omega)$ is the Bose population factor $[\exp(hc\omega/kT) - 1]^{-1}$. The quantities $\delta C^2/C^2$ and λ reflect the relative mean-square spatial fluctuations of the photoelastic and elastic constants, respectively. Since the MB model has been developed to describe light scattering from long-wavelength acoustic phonons, the frequency range in which Eqs. (2) and (3) are applicable is defined by the relation $(2\pi c\omega/v_\mu)\sigma < 1$, where $\mu = l, t$.

From Eqs. (2) and (3) the depolarization spectrum[15] $[\rho(\omega)]$ for the wave-vector nonconserving scattering can be shown to be

$$\rho(\omega) = \frac{I_{\parallel\perp}}{I_{\perp\perp}} = \left[\frac{4}{3} + \frac{10}{\frac{2}{3} + g_t/g_l}\left(\frac{\delta C_t^2 + \lambda C_l^2}{\delta C_t^2 + \lambda C_t^2}\right)\right]^{-1}\ . \quad (4)$$

The depolarization ratio of light scattering from optic modes has been shown to depend on mode symmetries, but for low-frequency light scattering $\rho(\omega)$ depends on the spatial fluctuations of the elastic and photoelastic constants.

At this point we note that comparison of Eqs. (1) and (2) is useful. In the low-frequency region the densities of states of both the transverse and longitudinal acoustic bands are proportional to ω^2. Thus, for low-frequency wave-vector nonconserving Stokes scattering we write

$$I_{\beta\alpha\gamma\delta} \propto C_{\beta\alpha\gamma\delta}(\omega)G(\omega)(1/\omega)[n(\omega)+1]\ , \quad (5)$$

where

$$C_{\beta\alpha\gamma\delta}(\omega) \propto x^2[g_t(x)E^t_{\beta\alpha\gamma\delta} + g_l(x)E^l_{\beta\alpha\gamma\delta}]\ , \quad (6a)$$

$$G(\omega) = \omega^2\ . \quad (6b)$$

The quantities x, g_t, g_l, E^t, and E^l are the same as defined in Eq. (3).

The experimentally obtained low-frequency Raman spectra can best be understood in terms of Eq. (5). In light of this expression, the low-frequency Raman spectra reduced by $[n(\omega)+1]/\omega$ are expected to exhibit an ω^4 frequency dependence at the lowest-frequency shifts. Since the light-scattering excess masks this frequency dependence at room temperature and is absent at low temperature, it is necessary to obtain low-temperature Raman spectra of the glasses to determine the frequency dependence of the quantity $C_{\beta\alpha\gamma\delta}(\omega)G(\omega)$. Figure 1 displays the analog low-temperature low-frequency Raman spectra of the glasses As_2S_3, GeS_2, $GeSe_2$, and As_2Se_3. The full Raman spectra of these glasses is presented elsewhere.[16] There is no evidence of a contribution due to the light-scattering excess (LSE) (the T dependence of LSE will be discussed in Sec. III B3). In Fig. 2 $I_{\perp\perp}\omega/[n(\omega)+1]$ is plotted versus ω on a log-log scale. The solid line in each of the traces has a slope of 4. Therefore the reduced low-frequency Raman spectra of the four glasses approaches an ω^4 frequency dependence as $\omega \to 0$. We have previously noted that for Se the density of vibrational states exhibited Debye character (i.e.,

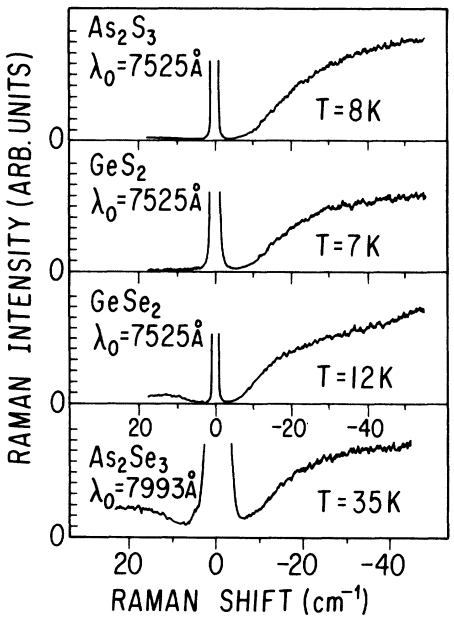

FIG. 1. Low-temperature, low-frequency, $\perp\perp$ Raman spectra of the chalcogenide glasses As_2S_3, GeS_2, $GeSe_2$, and As_2Se_3. Low-frequency spectra presented here and in all subsequent figures were recorded with a spectral slit width of $\sim 0.9\ \mathrm{cm}^{-1}$. In addition, all analog spectra though marked in cm^{-1} are displayed with abscissas that are linear in wavelength.

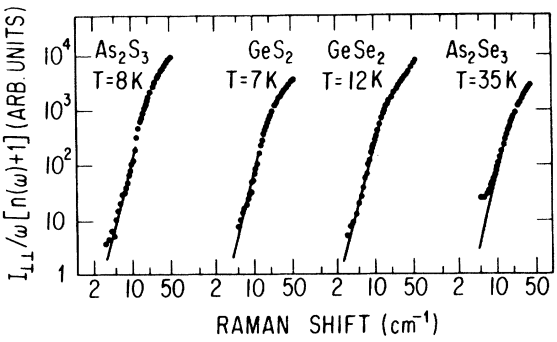

FIG. 2. $I_{\perp\perp}\omega/[n(\omega)+1]$ spectra of the glasses As_2S_3, GeS_2, $GeSe_2$, and As_2Se_3. The solid lines have a slope of 4.

ω^2 dependence) up to ~50 cm^{-1}.[22] Therefore on the basis that the density of states for the chalcogenide glasses studied here also show an ω^2 frequency dependence, we conclude that $C_{\beta\alpha\gamma\delta}$ exhibits an ω^2 frequency dependence as $\omega \to 0$. The above result is consistent with the results reported by Lannin who studied low-frequency scattering from a-Si films.[4] In previous investigations of the low-frequency Raman spectra of the bulk glasses Se,[7] As_2O_3,[6] and fused silica,[8] an ω^2 dependence of $C_{\beta\alpha\gamma\delta}$ was not observed. For the case of Se which apparently exhibits a long SCR,[7] the dependence would occur at a much lower frequency and thus be masked by the Rayleigh and scattered-light components. The expected ω^2 dependence was not observed in As_2O_3 probably as a result of insufficient resolution and a strong scattered-light component. In fused silica the light-scattering excess masked the ω^2 dependence of $C_{\beta\alpha\gamma\delta}$.[8] Therefore we suggest that in the limit of $\omega \to 0$ the ω^2 frequency dependence of $C_{\beta\alpha\gamma\delta}$ is a general property of light scattering from disordered solids.

Now that the lowest frequency limit of the MB model has been shown to be consistent with observation, the full result of the model can be explored. From Eqs. (3) and (6) the Raman coupling constant for $\|\perp$ scattering is

$$C_{\|\perp}(\omega) = A\omega^2[3(v_l/v_t)^5 e^{-[(2\pi c\omega)^2/v_l^2]\sigma^2} + 2e^{-[(2\pi c\omega)^2/v_t^2]\sigma^2}], \quad (7)$$

where A is a constant. Since v_l and v_t can be obtained from other measurements, only the parameters A and σ are unknown. As an example of the use of the model we show in Fig. 3 the digitally acquired low-frequency $\|\perp$ Raman spectra of As_2S_3 and the coupling constant $C_{\|\perp}$ obtained from the data. The solid line is a least-squares fit to the data using Eq. (7). The fit for $\omega < 30$ cm^{-1} is good while a strong deviation from the data is observed at $\omega > 30$ cm^{-1}. For this fit of Eq. (7) to the data a value of σ was obtained that indicated that the

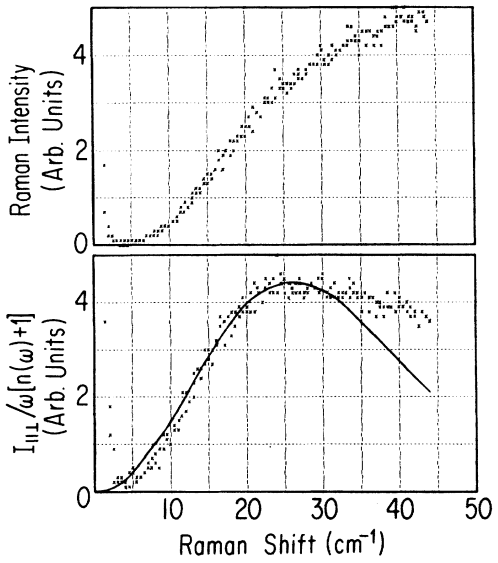

FIG. 3. Digital $\|\perp$ Raman (a) and $I_{\|\perp}/\omega[n(\omega)+1]$; (b) spectra of As_2S_3 at a temperature of 8 K. The solid line is a fit to the data using Eq. (7).

long-wavelength limit [defined by $(\sigma/v_t)2\pi c\omega < 1$] [2] applies only for $\omega < 32$ cm^{-1}. Therefore the deviation occurs where the MB model is no longer expected to apply.

In the preceding example the $\|\perp$ configuration was used to obtain the SCR because $C_{\|\perp}$ can be expressed in terms of only two unknowns as shown in Eq. (7). However the $C_{\perp\perp}$ spectrum cannot be described theoretically without the use of a third parameter. This difference will be discussed more completely in Sec. III A2.

2. *Determination of the structural correlation range*

In Sec. III A1 the MB model which is parametrized in terms of the SCR and the velocities of transverse and longitudinal acoustic waves, has been shown to describe the low-frequency light scattering from glasses. Therefore to determine the value of the SCR from the low-frequency Raman spectra, the velocities of transverse and longitudinal acoustic waves must be known. One method of obtaining v_l and v_t is from the Brillouin spectra of the wave-vector conserving scattering.[30] Figure 4 shows the room-temperature $\perp\perp$ Brillouin spectra of all the glasses studied in this report except As_2Se_3 (which does not transmit either 7993- or 7525-Å radiation at room temperature) and $(As_2S_3)_{0.5}(GeS_2)_{0.5}$. The peaks observed in the $\perp\perp$ Brillouin spectra are attributed to scattering from longitudinal acoustic modes.[30] The $\|\perp$ Brillouin spectra is expected to show only the transverse acoustic modes. In this polarization configuration only the

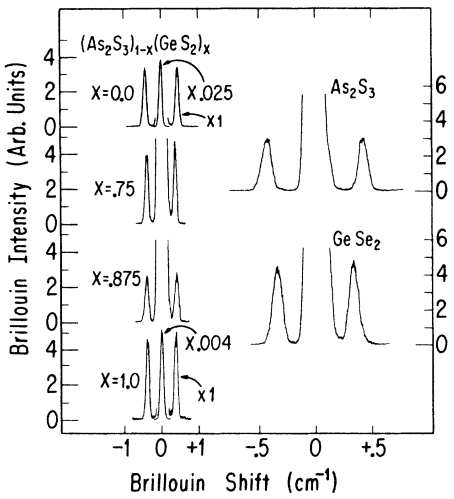

FIG. 4. Polarized ⊥⊥ 90° Brillouin spectra of As_2S_3, $GeSe_2$, GeS_2, $(As_2S_3)_{0.25}(GeS_2)_{0.75}$ and $(As_2S_3)_{0.125}(GeS_2)_{0.875}$.

peak at $\omega = 0$ due to Rayleigh and parasitic scattering was observed. The anomalously weak intensity of the transverse peak will be discussed further in Sec. IIIA3. The observed Brillouin shifts for the longitudinal acoustic modes of the glasses are listed in Table I. The velocity of longitudinal acoustic waves was determined from the Brillouin shifts following a method described elsewhere.[22] While the velocity of transverse acoustic waves was not obtainable from the Brillouin spectra, there have been ultrasonic determinations of v_l and v_t for the glasses As_2S_3 and As_2Se_3. In addition a recent interferrometric Brillouin measurement of GeS_2 has yielded v_l and v_t for that glass. The values of v_l and v_t from all measurements are also indicated in Table I.

In the previous section an expression [Eq. (7)] was given for the $C_{\parallel\perp}$ for low-frequency Raman spectra. The coupling coefficient for ⊥⊥ scattering can be obtained from Eqs. (1), (2), (5), and (6) and is found to be

$$C_{\perp\perp} = A\omega^2[2(v_l/v_t)^5 e^{-[(2\pi c\omega)^2/v_t^2]\sigma^2} + (15V + \tfrac{2}{3})e^{-[(2\pi c\omega)^2/v_t^2]\sigma^2}], \quad (8a)$$

where

$$V = [(\delta C_l^2 + \lambda C_l^2)/(\delta C_t^2 + \lambda C_t^2)]. \quad (8b)$$

The quantity V cannot be measured directly, but since it occurs in Eq. (4) which defines the depolarization spectrum, V can be determined from the experimentally obtained depolarization. Thus both the $\parallel\perp$ and ⊥⊥ scattering configurations can be used to determine the SCR. This fact is important since the ⊥⊥ scattering intensity is often greater than the $\parallel\perp$ scattering intensity by more than a factor of 2.[15,16]

We now apply Eqs. (7) and (8) to the low-frequency Raman spectra of the glasses As_2S_3, GeS_2, $GeSe_2$, and As_2Se_3. Figures 5–8 display the indicated experimentally determined coupling coefficients and the fit to the data using Eq. (7) or (8) depending on the scattering configuration. In all the ⊥⊥ fits the value of V was obtained using Eqs. (4) and (8b) and the experimentally determined depolarization ratio at the frequency of the maximum in the coupling-constant spectrum. The velocity of transverse acoustic waves for the $GeSe_2$ glass was obtained from the Brillouin spectra by assuming that the ratio v_l/v_t is the same for both GeS_2 and $GeSe_2$. This approximation may be justified by the fact that v_l/v_t is approximately the same for the glasses As_2S_3,[31] and As_2Se_3,[32] which have similar local structures.[14] The values of the SCR are summarized in Table II. We note that in each case the values obtained from ⊥⊥ and $\parallel\perp$ configurations are equal within the limits of the assigned error. In addition the low-temperature and room-temperature measurements yield approximately equivalent results.

The above discussion describes a method of obtaining the SCR from the low-frequency Raman

TABLE I. Brillouin shifts and velocities of sound of As-Ge-S-Se glasses.

Glass	90° Brillouin[a] shift (cm^{-1})	This work v_l[b] (10^5 cm/sec)	Other measurements v_t (10^5 cm/sec)	v_l (10^5 cm/sec)	Reference
As_2S_3	0.420	2.63	1.40	2.56	31
GeS_2	0.375	2.95	1.75	2.99	22
$GeSe_2$	0.337	2.21	...	...	...
As_2Se_3	...	...	1.22	2.26	32
$(As_2S_3)_{0.25}(GeS_2)_{0.75}$	0.377	2.68	...	...	...
$(As_2S_3)_{0.125}(GeS_2)_{0.875}$	0.399	2.96	...	...	...

[a] Estimated accuracy ± 0.009 cm^{-1}.
[b] Estimated accuracy ± 0.09 × 10^5 cm/sec.

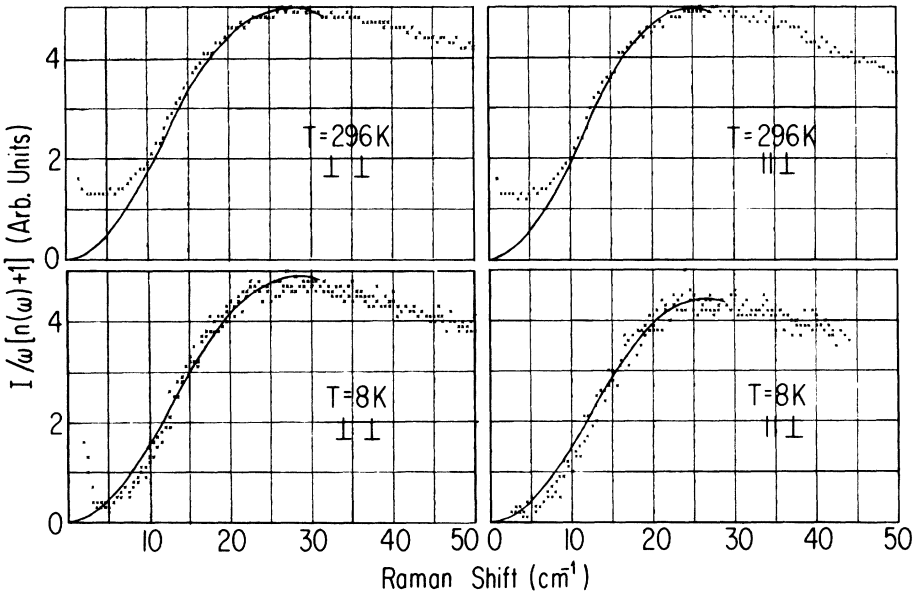

FIG. 5. Polarized $I/\omega[n(\omega)+1]$ spectra of As_2S_3. The solid lines are fits to the data using Eq. (7) ($\|\perp$) and Eq. 8(a) ($\perp\perp$).

spectra of glasses by curve fitting either Eq. (7) or (8) to $I/\omega[n(\omega)+1]$. Simple considerations indicate that an approximately equivalent result can be obtained from the position of the "boson peak"[33] (the characteristic peak in the low-frequency Raman spectra of disordered solids) in the room-temperature Raman spectrum. At room temperature the term $[n(\omega)+1]/\omega$ is approximately proportional to ω^2 in the low-frequency region.[2-4] Thus from Eqs. (5) and (6) $I \propto C(\omega)$. The similarity of the $I_{\perp\perp}$ Raman spectra of $GeSe_2$ and the $I_{\perp\perp}/\omega[n(\omega)+1]$ is demonstrated in Fig. 9. In addition, the function $\omega^2 e^{-(2\pi c\omega\sigma/v)^2}$ has a maximum at $\omega = v/2\pi c\sigma$. Thus for $\|\perp$ scattering where the intensity is dominated by the contribution from the transverse acoustic modes, the SCR can be approximately obtained from the relation

$$2\sigma \simeq v_t/\pi c\omega_{\text{peak}}^{\|\perp}. \tag{9}$$

Here $\omega_{\text{peak}}^{\|\perp}$ is the frequency shift of the boson peak. For the case of the $\perp\perp$ Raman configuration, the contribution to the scattering intensity from longitudinal and transverse modes is approximately equal. Thus the SCR can be obtained from the relation

$$2\sigma \simeq \bar{v}/\pi c\omega_{\text{peak}}^{\perp\perp}. \tag{10}$$

Here $\omega_{\text{peak}}^{\perp\perp}$ is the frequency shift of the boson peak in the $\perp\perp$ configuration, and $\bar{v}$ is the average of the transverse and longitudinal velocity of acoustic waves. The SCR of As_2S_3, GeS_2, and $GeSe_2$ obtained from the "boson peak" frequency shift and Eqs. (9) and (10) as they apply are listed in Table

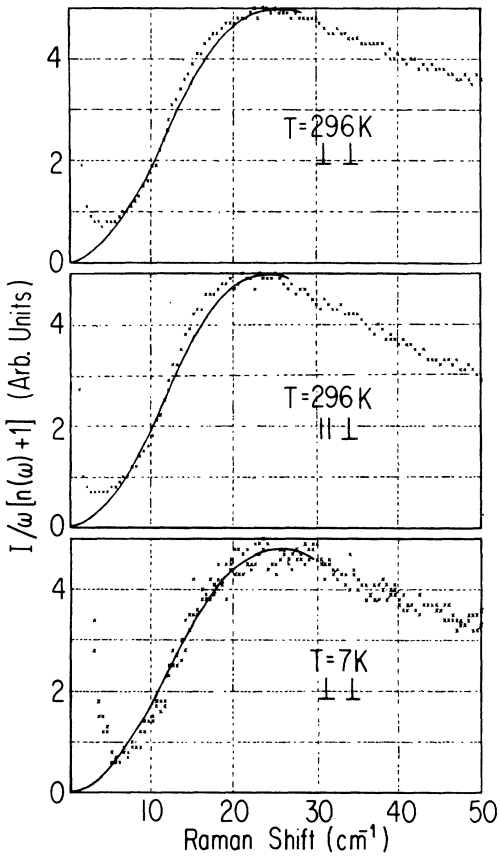

FIG. 6. Polarized $I/\omega[n(\omega)+1]$ spectra of GeS_2. The solid lines are fits to the data using Eq. (7) ($\|\perp$) and Eq. (8a) ($\perp\perp$).

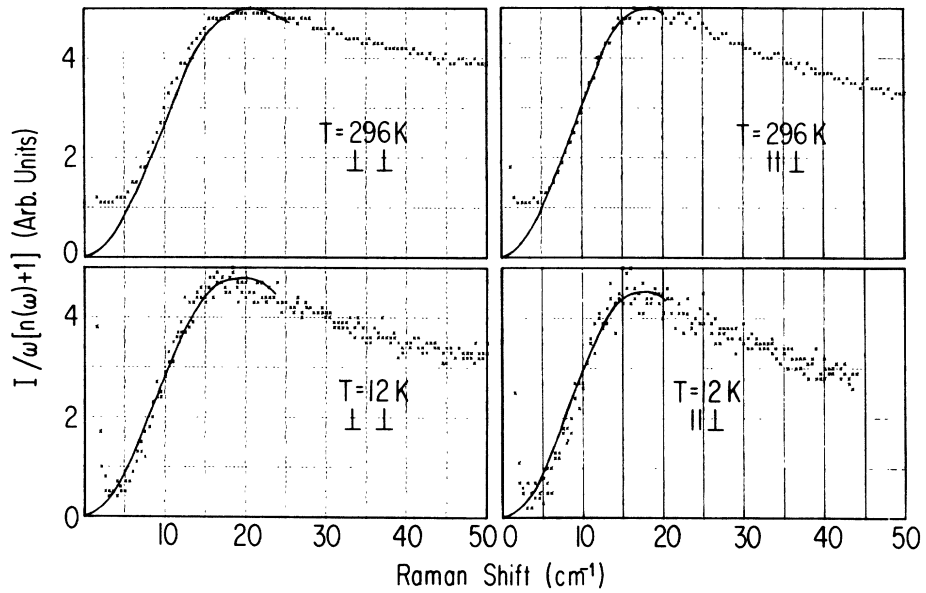

FIG. 7. Polarized $I/\omega[n(\omega)+1]$ spectra of $GeSe_2$. The solid lines are fits to the data using Eq. (7) ($\|\perp$) and Eq. (8a) ($\perp\perp$).

II. As can be seen the values determined from the $I_{\perp\perp}$ spectra yield SCR's slightly larger than the SCR obtained from curve fitting while the SCR obtained from the $I_{\|\perp}$ spectra yield slightly smaller values.

3. *Depolarization predictions*

The depolarization of light scattered at the frequency of the "boson peak" has been used in the previous section to obtain the SCR. In this section the prediction of the MB model for the depolarization spectrum of low-frequency light scattering is explored.

Martin and Brenig have suggested that for a-Si $\delta C_l/C_l \approx \delta C_t/C_t$.[2] With this approximation Eq. (4) becomes

$$\rho(\omega)=\frac{I_{\|\perp}}{I_{\perp\perp}}=\left[\frac{4}{3}+\frac{10}{\frac{2}{3}+g_t/g_l}\left(\frac{C_l^2}{C_t^2}\right)\right]^{-1}. \tag{11}$$

They have also shown that this approximation yields a depolarization spectrum consistent with that observed for a-Si films. Winterling has used an expression equivalent to Eq. (11) to interpret the depolarization spectrum of low-frequency light scattering from fused silica.[8] For the case of fused silica, Eq. (11) gives reasonable agreement with the observed depolarization at the lowest frequencies (i.e., $\omega<5$ cm^{-1}), but at higher frequencies (which are still within the long-wavelength limit) there is a considerable discrepancy.[22]

To apply Eq. (11) to the observed low-frequency depolarization spectrum for the chalcogenide glasses, the value of C_l/C_t must be obtained. Using Eq. (3j) and the fact that $p_{44}=\frac{1}{2}(p_{11}-p_{12})$, we find

$$C_l/C_t=\tfrac{1}{2}p_{12}/p_{44}+\tfrac{1}{3}. \tag{12}$$

The ratio p_{12}/p_{44} can be obtained from the ratio of the intensities of the Brillouin peaks and the ratio v_l/v_t using the following equation[30]:

$$|p_{44}/p_{12}|=\sqrt{2}\,(v_t/v_l)(I_t/I_l)^{1/2}. \tag{13}$$

Here I_l and I_t are the intensities of the Brillouin peaks arising from longitudinal and transverse acoustic waves, respectively. Also, Eq. (13) applies for the 90° scattering configuration, with I_l observed in the $\perp\perp$ configuration while I_t is seen in the $\|\perp$ (or $\perp\|$) configuration.[30]

While the Brillouin measurements presented here do not exhibit the transverse acoustic mode,

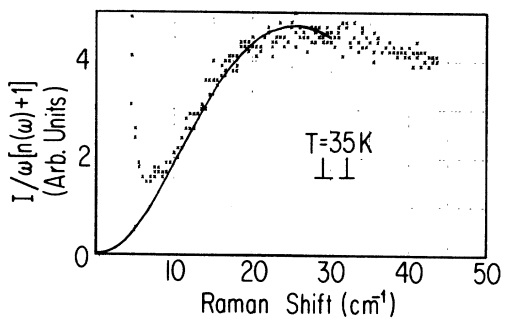

FIG. 8. Polarized $I/\omega[n(\omega)+1]$ spectrum of As_2Se_3. The solid line is a fit to the data using Eq. (8a).

TABLE II. Structural correlation ranges (2σ) of binary chalcogenide glasses determined for different configurations and by different methods. The indicated errors were determined from the quality of the fit to the data or from the uncertainty in the position of the "boson peak."

Glass	Temperature (K)	2σ (Å) Curve fitting $\parallel \perp$	Curve fitting $\perp\perp$	"Boson peak" $\parallel \perp$	"Boson peak" $\perp\perp$
As_2S_3	296	6.5±0.8	6.8±0.8	5.7±0.8	7.3±0.8
	8	6.3	6.6	...	...
GeS_2	296	8.2	8.6	8.25	10.5
	7	...	8.6	...	...
$GeSe_2$	296	8.4	8.7	8.1	9.5
	8	8.6	9.1	...	...
As_2Se_3	35	...	6.1	...	...

a lower limit to the ratio I_l/I_t can be established. Our measurements suggest that $I_l/I_t \geq 40$ for As_2S_3 and $GeSe_2$. For GeS_2 the ratio I_l/I_t has been determined from interferometric Brillouin measurements and found to be ~40. In addition the photoelastic constants p_{11} and p_{12} of As_2S_3 have been recently measured by piezobirefringence methods.[34] The results of this measurement are $p_{11}=0.25$ and $p_{12}=0.24$ and indicate [by use of Eq. (13)] that $I_l/I_t \approx 1350$. While a small error in the measurement of either p_{11} or p_{12} could change I_l/I_t significantly, the Brillouin peak from the transverse acoustic mode would probably still be too weak to observe with the instrument used here.

We note that a lower limit of the ratio I_l/I_t establishes a lower limit of C_l/C_t. Consequently, from examination of Eq. (11), the value obtained for C_l/C_t sets an upper limit of the depolarization ratio. The solid lines in Figs. 10(a)–10(c) represent the theoretical depolarization spectra of As_2S_3, GeS_2, and $GeSe_2$, respectively, obtained from Eq. (11) and the ratio C_l/C_t determined assuming $I_l/I_t=40$. Clearly the results do not agree with the observed depolarization spectra, although both theoretical and observed depolarization spectra decrease with increasing Raman shift.

We have suggested that the quantity V as defined in Eq. (8b) be treated as a variable to be determined from the experimentally observed depolarization. The depolarization spectrum is then given by

$$\rho(\omega)=\frac{I_{\parallel\perp}}{I_{\perp\perp}}=\left(\frac{4}{3}+\frac{10V}{\frac{2}{3}+g_t/g_l}\right)^{-1}. \tag{14}$$

The dashed lines in Figs. 10(a)–10(c) indicate the theoretical depolarization spectra obtained using Eq. (14) and the values of V determined as described in Sec. III A2. In this case, also, Eq. (14) does not fit the experiment. Nevertheless, the use of Eq. (8) to extract the SCR is still justified for two reasons: First, $C_{\perp\perp}$ does not vary strongly with V; second, with the choice of V as described, the theoretical depolarization ratio is still within ±15% of the experimentally determined ρ over the frequency region of interest.

4. *Structural implications of other measurements*

Structural correlations in glasses can be inferred from x-ray, scattering results, and from Raman spectra of optic vibrational modes.[35] In this section we compare the SCR obtained from low-frequency light scattering to that obtained from other methods. In addition, the results obtained in this study are discussed in terms of the amorphous structure of the glasses.

It has recently been suggested by de Neufville *et al.*,[36] that the structural correlations of amorphous materials can be approximately determined

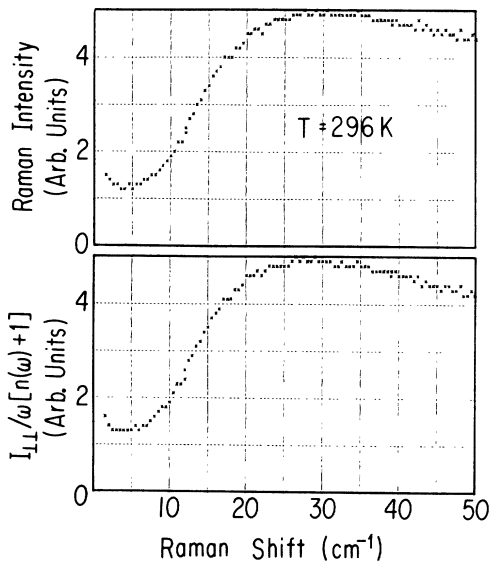

FIG. 9. Polarized Raman and $I_{\perp\perp}/\omega[n(\omega)+1]$ spectra of As_2S_3.

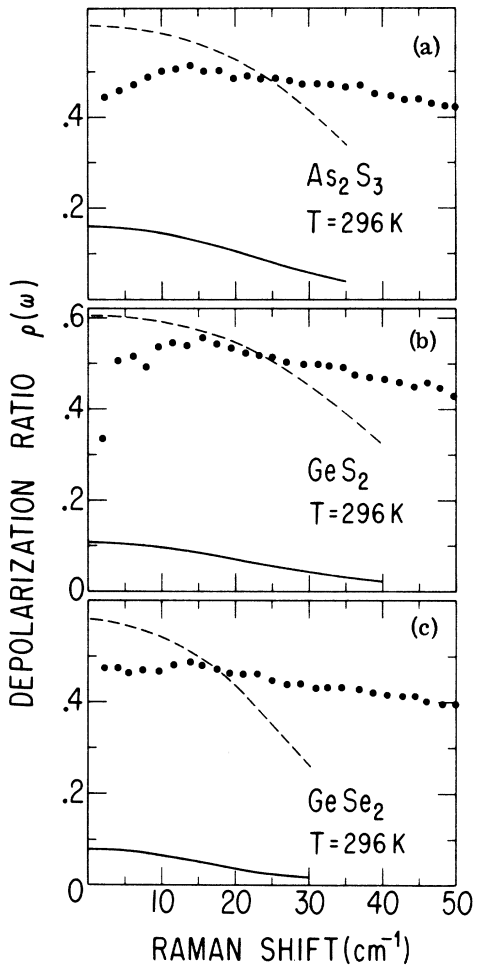

FIG. 10. Depolarization spectra of As_2S_3, GeS_2, and $GeSe_2$. The solid lines represent the theoretical values using Eq. (11). The dashed lines are plots of Eq. (14) with the quantity V scaled to yield agreement with the experimental $\rho(\omega)$ at the frequency shift of the "boson peak."

by applying the Scherrer equation to the first peak in the x-ray diffraction spectrum. This equation has been generally used to determine the size of microcrystallites.[37] The form of the Scherrer equation to be used for amorphous materials as given by de Neufville *et al.* is

$$L = 0.9\lambda/B(2\phi)\cos\phi\,, \tag{15}$$

where λ is the x-ray wavelength, ϕ is the scattering angle of the peak intensity, $B(2\phi)$ is the full width at half maximum (in radians), and L is an indication of the length of structural correlations.

The x-ray diffraction spectra of amorphous samples of GeS_2,[38] As_2S_3,[36] and As_2Se_3,[36] have been reported. We have applied Eq. (15) to these reported spectra and find SCR's of 14 ± 2, 19 ± 3, and 17 ± 3 Å for GeS_2, As_2S_3, and As_2Se_3, respectively. There are however to our knowledge no x-ray diffraction measurements of $GeSe_2$, but Fawcett *et al.*[39] have measured the electron diffraction spectra of $GeSe_2$ films. While the Scherrer formula should be applicable to electron diffraction spectra also, because of the strong dependence of electron scattering factors, meaningful peak widths could not be extracted from the data of $GeSe_2$.[40] Though the values of the structural correlations obtained from application of the Scherrer equation to the first peak in the x-ray diffraction spectra are within a factor of 3 of the SCR obtained from low-frequency light scattering, we suggest that either the x-ray Scherrer method does not describe the structural correlations in amorphous materials or alternatively reflects correlations different from those treated in the MB model.

As mentioned previously, Raman spectra of the optic modes of glasses have been described in terms of the normal vibrations of local atomic clusters. Thus by identifying the atomic clusters that determine the optic vibrational spectra of the glasses, the diameter of the atomic cluster can be associated with the SCR. Therefore one might assign a SCR equal to the diameter of the pyramidal $AsS_3(Se_3)$ unit for $As_2S_3(As_2Se_3)$ and the tetrahedral $GeS_4(Se_4)$ unit for $GeS_2(GeSe_2)$. The appropriate SCR following the above reasoning would be ~3.5 to ~5 Å for all four glasses. Recently however strong features have been observed in the Raman spectra of $GeSe_2$ and GeS_2 that cannot be attributed to the normal vibrations of the $GeSe_4$ or GeS_4 tetrahedral units.[41] These features have been identified as arising from ring structures.[41] The ring structures are composed of six Ge atoms interconnected by S or Se atoms to form a simply connected ring. The diameter of such a ring is approximately 7–8 Å. A correlation range of this size is in excellent agreement with the SCR of GeS_2 and $GeSe_2$ obtained from the low-frequency light-scattering measurements.

To date there have been no experiments to our knowledge that demonstrate that ringlike structures contribute strongly to the vibrational spectrum of either As_2S_3 or As_2Se_3. The crystal structure of orpiment (crystalline As_2S_3) exhibits ringlike structures of diameter ~7 Å,[42] thus we expect similar but distorted ring structures to exist in both As_2S_3 and As_2Se_3 glasses. Because the SCR obtained here for As_2S_3 and As_2Se_3 is ~6.5 Å it is possible that ringlike structures also contribute to the vibrational spectra of these glasses. Whether this is the case or not we suggest that the SCR of ~6.5 Å implies that structures larger than the AsS_3 or $AsSe_3$ pyramidal units must be considered to fully describe the vibrational properties of the glasses.

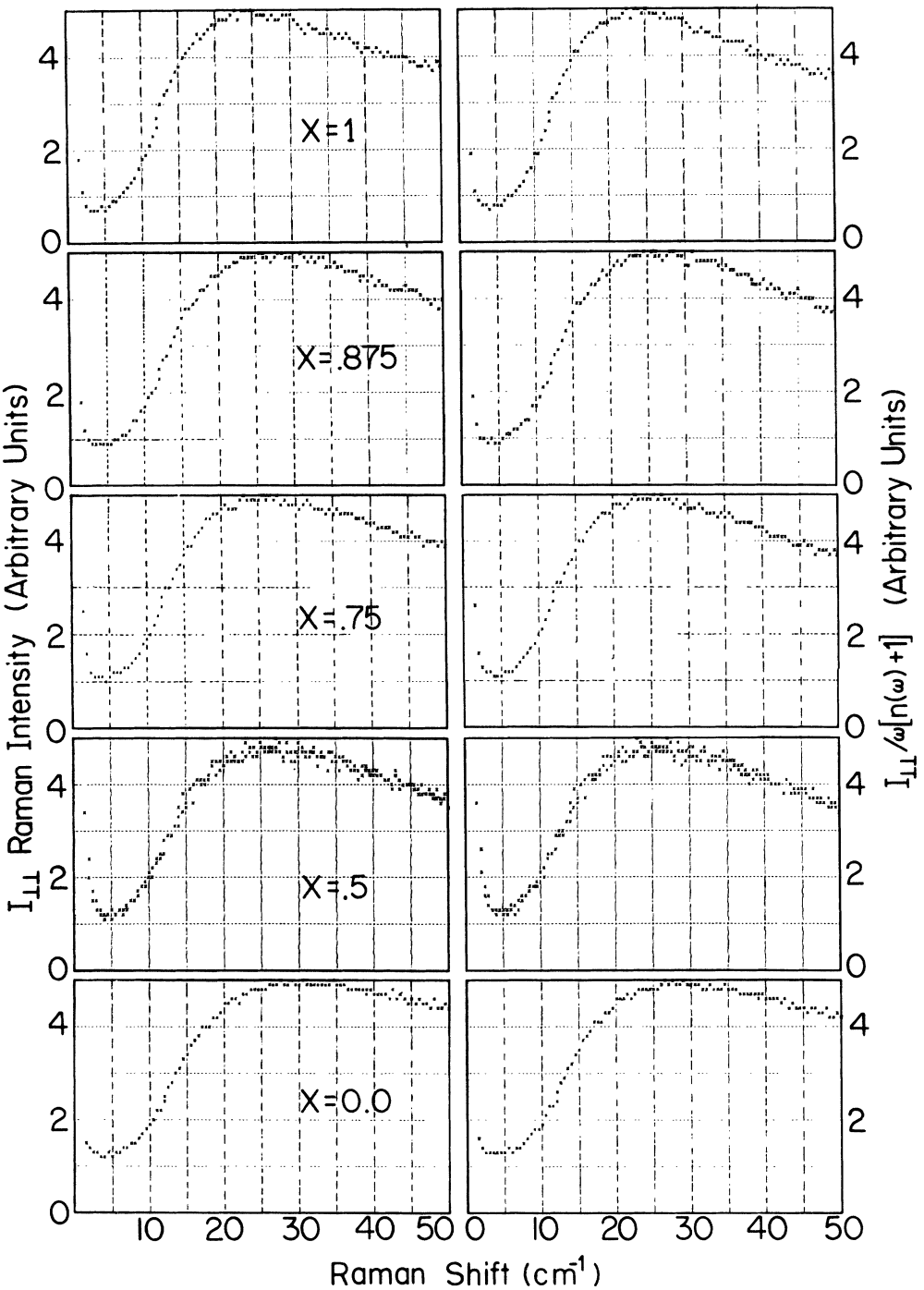

FIG. 11. Digital $\perp\perp$ Raman and $I_{\perp\perp}/\omega[n(\omega)+1]$ spectra of the glass alloy series $(As_2S_3)_{1-x}(GeS_2)_x$.

5. *Alloys*

Since the SCR is sensitive to differences in the amorphous structure, the alloy system of $(As_2S_3)_{1-x}(GeS_2)_x$ will be discussed. The digital room-temperature, low-frequency $\perp\perp$ Raman spectra and the $I_{\perp\perp}/\omega[n(\omega)+1]$ spectra of the $x=0$, 0.5, 0.75, 0.875, and 1.0 members of the alloy are displayed in Fig. 11. (The full Raman spectra of these alloys have been presented elsewhere.[43]) Unfortunately there are no measurements of v_t for the alloys $x=0.5$, 0.75, and 0.875, therefore v_t

has been estimated from v_l obtained from the Brillouin measurements for the $x=0.75$ and 0.875 alloy samples. To accomplish this the ratio v_l/v_t was assumed to vary linearly with the ratio of the concentrations of As and Ge atoms. Also for the $x=0.5$ alloy no Brillouin spectrum was obtained, thus both v_l and v_t were extrapolated from the values of the $x=0.75$ alloy and As_2S_3 ($x=0$). The SCR of all the alloys has been determined using Eq. (10) and the extrapolations for v_t. The results are summarized in Table III. The SCR's obtained for the $x=0.5$, 0.75, and 0.875 samples are approximately equal, and the values are between the 7.5-Å SCR of As_2S_3 and the 10.5-Å SCR of GeS_2 obtained from the position of the "boson peak."

The bonding structure of the alloys is different from that of the binary chalcogenide glasses in that two different types of bonds, As-S and Ge-S, are present in the former. The alloys exhibit a pseudobinary nature and are composed of only AsS_3 pyramidal units and GeS_4 tetrahedral units.[16] Thus while the local atomic structures of the alloys are identifiable, it is difficult to determine what other larger structures are of importance. In addition the large uncertainty in the SCR due to the lack of measured values of v_l and v_t makes interpretation of these results difficult at this time.

B. Light-scattering excess

1. Aspects of the models

We have demonstrated that spectral features in low-frequency Raman spectra that arise from scattering from long-wavelength acoustic phonons can be identified, therefore the light-scattering excess (LSE) can be studied more readily. Recently Theodorakopoulos and Jäckle[27](TJ) have proposed a model to describe the low-frequency light scattering from defects in glasses. They have successfully applied their model to describe the existence and temperature dependence of the LSE observed in fused silica.[8] The TJ model is similar but more detailed than the model presented by Winterling[8] to describe the LSE. In the following we will briefly describe the results of both models.

The existence of two-level defect states which have been postulated to be responsible for the linear T-dependent term observed in the low-temperature specific heat of glasses,[12,13] is the major assumption of both models. These defects can decay or be excited in two ways; by quantum-mechanical tunneling, or by thermally activated jumping across across the barriers. The case of quantum-mechanical tunneling involves resonant absorption or emission of a phonon. The quantum-mechanical tunneling mechanism occurs at low temperatures. At higher temperatures oscillator levels are filled and thermally activated jumping across the barrier becomes the dominant decay mechanism.

The Winterling model suggests that the thermally activated decay produces a low-frequency tail in the spectral profile of acoustic phonons. When $\omega_0\tau \gg 1$, where ω_0 is the phonon frequency and τ is the characteristic relaxation time, a central mode occurs with full width at half maximum of approximately $2\tau^{-1}$. Light can then couple to the central mode and cause the observed LSE. This form of scattering has been attributed to indirect coupling because it occurs through phonon tails.

The TJ model assumes that the two state defects exhibit different electric polarizability, and the specific state of a defect can be defined by a pseudospin variable S_j^z which has values $\pm\frac{1}{2}$. The polarizability difference of the two levels of the jth defect state can be written in diagonal form as

$$\begin{pmatrix} \Delta\alpha_j^{(1)} & 0 & 0 \\ 0 & \Delta\alpha_j^{(2)} & 0 \\ 0 & 0 & \Delta\alpha_j^{(3)} \end{pmatrix}, \tag{16}$$

Thus the time dependence of the fluctuation of the polarizability is

$$\Delta\alpha_j^{(i)}(t) = \Delta\alpha_j^{(i)} S_j^z(t). \tag{17}$$

For the case when $\Delta\alpha^{(1)} = \Delta\alpha^{(2)} = 0$ and $\Delta\alpha^{(3)} = \Delta\alpha$ TJ find

$$\frac{I_{ll}(\omega)}{\omega[n(\omega)+1]} \propto \frac{(\Delta\alpha)^2}{2\pi kT} \int dV\, P(V) \frac{\tau(V)}{1+\omega^2\tau^2(V)}, \tag{18}$$

TABLE III. Structural correlation ranges (2σ) of the alloy system $(As_2S_3)_{1-x}(GeS_2)_x$.

x	$z=\frac{x}{2-x}$	v_t (10^5 cm/sec)	v_l (10^5 cm/sec)	2σ (Å)
1.0	1.0	1.75	2.99	10.5±0.8
0.875	0.778	1.69[a]	2.93	9.1
0.75	0.60	1.64[a]	2.88	9.4
0.5	0.33	1.56[a]	2.81[a]	8.9
0	0	1.47	2.72	7.3

[a] Extrapolated value.

where

$$\tau^{-1} = \tau_0^{-1} e^{-V/T},$$
$$P(V) = \bar{P} \exp[-(V - V_m)^2/V_0^2]. \tag{19}$$

Here V, V_m, and V_0 are, respectively, the potential barrier height, the most likely value of V, and the width of the distribution of V. The quantities $\bar{P}$ and τ_0 are constants and k is the Boltzmann constant. In addition the depolarization spectrum of the LSE has been found by TJ to be

$$\rho = I_{\parallel\perp}/I_{\perp\perp} = \tfrac{1}{2}[(\gamma - 1)/(1 + \tfrac{2}{3}\gamma)], \tag{20}$$

where

$$\gamma = 3\left(\sum_{i=1}^{3} \Delta\alpha^{(i)2}\right) \Big/ \left(\sum_{i=1}^{3} \Delta\alpha^{(i)}\right)^2. \tag{21}$$

The TJ model has been applied successfully to describe the temperature dependence of the LSE of fused silica using Eq. (8) together with ultrasonic determinations of the values of τ_0, $\bar{P}$, V_m, and V_0. In addition the approximation $\Delta\alpha_j^{(3)} = \Delta\alpha$ and $\Delta\alpha_j^{(1)} = \Delta\alpha_j^{(2)} = 0$ yields a depolarization ratio for the LSE of $\frac{1}{3}$ which is in agreement with the observed value 0.30 ± 0.03.[8] While the Winterling model does not describe the temperature dependence or the depolarization explicitly, Winterling suggests that since the LSE arises from tails of the acoustic modes the value of the depolarization of both should be approximately equal. For fused silica this is as observed.

The previous discussion applies for sample temperatures greater than 10 K. For lower temperatures quantum-mechanical tunneling is important. The TJ model addresses the problem of light scattering directly from the quantum states. The polarization anisotropy $\Delta\alpha_j(t)$ is an operator in this case. TJ note that $\Delta\alpha_j(t)$ can also be written in a pseudospin formalism as

$$\Delta\alpha_j(t) = \sum_{\mu=1}^{3} \Delta\alpha_j^{\mu} S_j^{\mu}(t). \tag{22}$$

For the case where $\Delta\alpha_j^{\mu} = \Delta\alpha$ independent of μ they find

$$\frac{I_{\perp\perp}(\omega)}{\omega[n(\omega)+1]} \propto (\Delta\alpha)^2 \frac{N(\omega)}{\omega} \tanh\left(\frac{\hbar\omega}{2kT}\right), \tag{23}$$

where $N(\omega)$ is the density of states of the defects. The proportionality constants for both Eqs. (18) and (23) are identical.[27] TJ find that for fused silica $I_{\perp\perp}(\omega)/\omega[n(\omega)+1]$ at 5-cm^{-1} shift should be approximately equal at 300 and 2 K. The high-temperature scattering arises from thermal activation which is described by Eq. (18) while the low-temperature scattering arises from quantum-mechanical tunneling which is described by Eq. (23).

In this section the LSE of the chalcogenide glasses

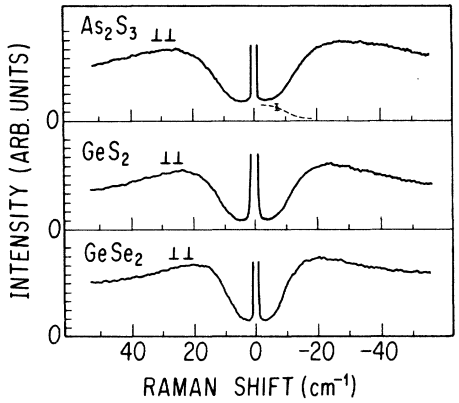

FIG. 12. Polarized room-temperature Raman spectra of As_2S_3, GeS_2, and $GeSe_2$. The dashed line in the As_2S_3 spectrum represents the contribution due to the LSE.

As_2S_3, GeS_2, $GeSe_2$, and the alloy system $(As_2S_3)_{1-x}(GeS_2)_x$ will be discussed. Figure 12 displays the analog room-temperature low-frequency Raman spectra of As_2S_3, GeS_2, and $GeSe_2$. All spectra exhibit an intensity at ~5 cm^{-1} which cannot be described in terms of scattering from Debye phonons. In addition the digital spectra of the alloy series shown in Fig. 11 also exhibit the excess scattering for all samples.

2. *Depolarization of the LSE*

The depolarization spectrum of the low-frequency light scattering is useful not only to describe the characteristics of the LSE but also to distinguish the Rayleigh, Brillouin, and parasitic scattered-light components from the LSE. Shown in Fig. 13 are the low-frequency Raman and depolarization spectra of As_2S_3 at $T = 8$ K and at room temperature. The feature at 0 frequency shift is predom-

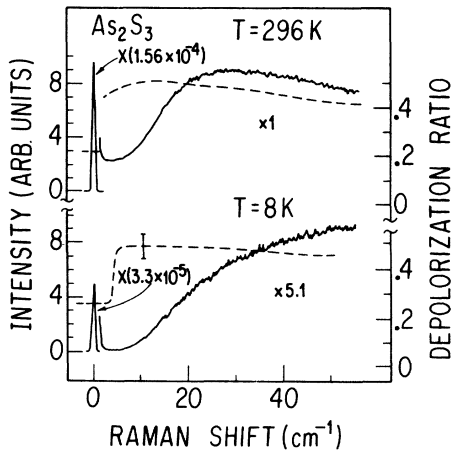

FIG. 13. ⊥⊥ Raman and depolarization spectra of As_2S_3 at 296 and 8 K.

inantly due to Rayleigh or parasitically scattered light. Since the depolarization of the room-temperature low-frequency Raman spectra at 5 cm^{-1} is approximately the same as that at 20 cm^{-1} and because the depolarization of the central component is much lower ($\rho_{\omega=0}=0.25$), we conclude that the LSE cannot be attributed to Rayleigh or parasitic scattered light. In addition since the ratio of the Brillouin components observed in the $\|\perp$ and $\perp\perp$ configuration is less than $\frac{1}{40}$, the LSE cannot be ascribed to high-frequency tails of the Brillouin peaks.

Winterling has noted that the room-temperature Raman spectrum of fused silica shows a slight increase or turn up as $\omega \to 0$ in the region $\omega < 10$ cm^{-1}.[8] This does not appear to be the case for any of the glasses studied here. From the fact that the scattering intensity at less than 5 cm^{-1} in the $T=8$ K Raman spectra exhibits the same depolarization as the $\omega=0$ component, it can be concluded that the turnup of the scattering intensity at ~4 cm^{-1} is due to the Rayleigh and scattered-light components. Therefore by comparing the profile of the scattering intensity at Raman shifts less than 5 cm^{-1} in the $T=296$ and 8 K spectra, we conclude that the turn up of scattering intensity of the $T=296$ K spectra below 5 cm^{-1} is not due to the LSE. Thus it appears that the Raman intensity for frequency shifts less than 7 cm^{-1} is approximately constant. This conclusion seems generally true for all the glasses studied here.

Consider now the depolarization of the LSE. As can be seen from Fig. 10, the LSE exhibits a depolarization similar to that of the "boson peak." This is consistent with the observed depolarization of fused silica and with recent measurements of the LSE for B_2O_3 and As_2S_3 glasses.[9] Since a particular value of the depolarization can be obtained from the TJ model using Eq. (21) by assuming that the tensor components of Eq. (16) are nonzero and different, the fact that for a large class of glasses the LSE has a depolarization equal to that of the boson peak suggests that the properties of the glass itself are manifested in the depolarization of the LSE. However the observed depolarization is also consistent with the suggestion of the Winterling model that the LSE arises from low-frequency tails of acoustic phonons.

3. *Temperature dependence of As_2S_3*

In this section the temperature dependence of the Raman spectra of As_2S_3 is examined. Arsenic trisulfide was chosen because its low-frequency Raman spectra exhibited the strongest LSE with respect to the "boson peak." The temperature dependence of the low-frequency and normal Raman spectra of As_2S_3 are shown in Figs. 14 and 15. The temperature dependence of the normal Raman spectra has been reported previously,[15] but it is shown here to put the low-frequency spectra in proper perspective. As is evidenced in Fig. 14, the scattering intensity at 5 cm^{-1} exhibits a much stronger temperature dependence than the other regions of the low-frequency Raman spectra.

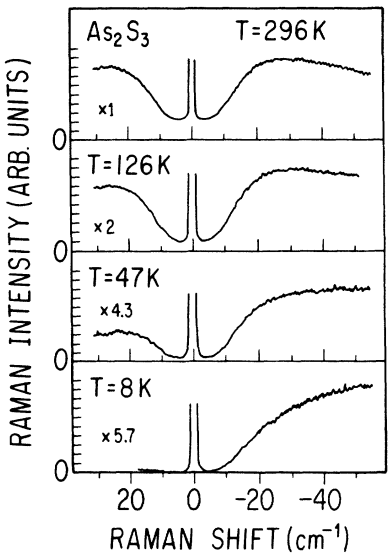

FIG. 14. Temperature dependence of the low-frequency $\perp\perp$ Raman spectra of As_2S_3.

The temperature dependence of the Raman spectra for several Raman shifts is plotted in Fig. 16. To obtain the data of Fig. 14 all spectra were intensity normalized by assuming that the intensity

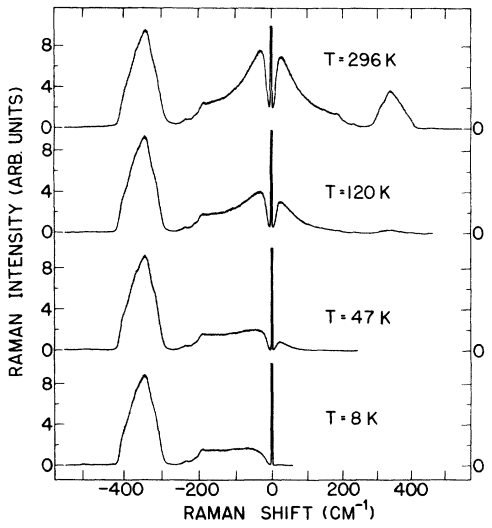

FIG. 15. Temperature dependence of the "normal" $\perp\perp$ Raman spectra of As_2S_3 recorded with a spectral slit width of ~3 cm^{-1}.

of the feature at ~340 cm^{-1} exhibits a temperature dependence proportional to $[n(\omega)+1]$.[19] The low-frequency spectra were normalized at 40 cm^{-1} again to $[n(\omega)+1]$ dependence after it was determined from the normal Raman spectra that the intensity at 40 cm^{-1} is consistent with this assumption. The solid lines in Fig. 16 describe the expected temperature dependence of the $T = 296$ K intensity (at the indicated frequency shift) if the scattering were due to boson excitations. Clearly the intensity at 5 cm^{-1} does not follow the $[n(\omega)+1]$ dependence. This result is consistent with the observed temperature dependence of the LSE of fused silica.[8] However the Raman intensity at 260 cm^{-1} also does not follow the expected temperature dependence. The dashed lines in Fig. 16 indicate the expected temperature dependence if the scattering were attributed to two-phonon summation processes. In addition the low density of states at $\omega = 2.5$ cm^{-1} also argues against this mechanism. As can be seen the observed temperature dependence at both 260 and 5 cm^{-1} cannot be attributed to two-phonon summation processes. Another possible two-phonon scattering mechanism that might account for the observed temperature dependence of the LSE is difference processes in which the phonon created and that annihilated are of approximately equal energy. For this case, if the two phonons have an energy of ~30 cm^{-1} then the ratio of the Raman intensity at 5 cm^{-1} for $T = 296$ and 47 K would be $I(296)/I(47) = 6.1$. The observed value of this ratio is 3.1 ± 0.2. In addition for phonons of higher energy, the predicted value of $I(296)/I(47)$ becomes larger. Thus we conclude that two-phonon differences processes are not responsible for the LSE. This conclusion also holds for fused silica.[8]

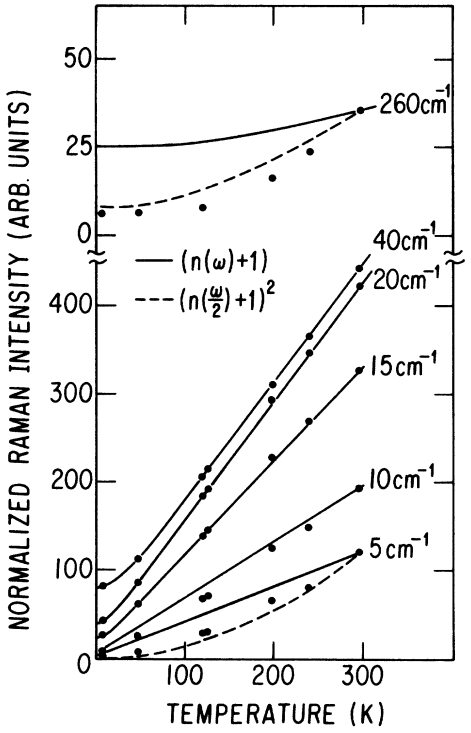

FIG. 16. Normalized temperature dependence of the Raman spectra of As_2S_3 at several different frequency shifts. The solid lines represent the expected dependence of first-order Raman scattering. The dashed lines represent the expected dependence of two-phonon summation Raman processes.

The similar temperature dependence of the scattering intensity at 5 and 260 cm^{-1} may lead to the assumption that the LSE extends past 240 cm^{-1}. However, in Sec. IIIB4 we show that the LSE is confined to Raman shifts of less than 20 cm^{-1}. Thus the "excess" at 260 cm^{-1} is probably due to tails of the optic phonons in the strong band at ~340 cm^{-1} and two phonon scattering.

While the LSE observed at room temperature may be attributed to thermal activation of the defects, the quantum-mechanical tunneling effects should occur at $T < 10$ K. Shown in Fig. 17 is the digital low-frequency Raman and $I_{\perp\perp}/\omega[n(\omega)+1]$ spectra of As_2S_3 recorded at a sample temperature of 2 K. There is no sign of a contribution resembling the LSE observed at room temperature. Thus we do not observe quantum-mechanical tunneling of the defect states. Since not all defects can exhibit the tunneling property, one possibility for this result is that the $\Delta\alpha$ (polarizability dif-

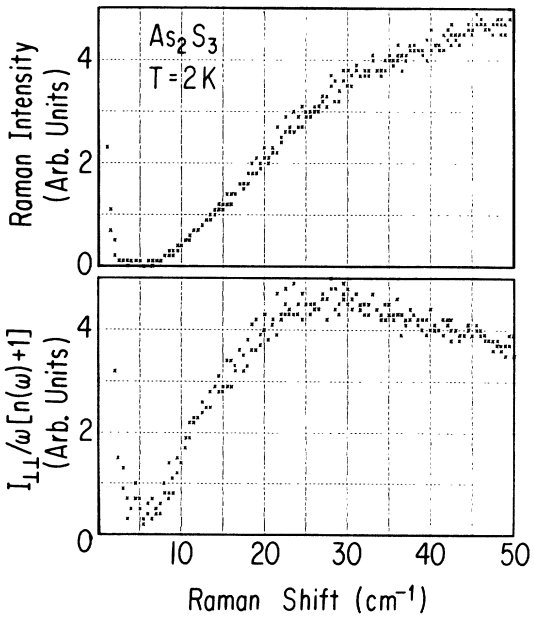

FIG. 17. Digital $\perp\perp$ Raman and $I_{\perp\perp}/\omega[n(\omega)+1]$ spectra of As_2S_3 recorded at a sample temperature of 2 K.

ference of the two states of the defect) is much smaller for states that exhibit quantum tunneling.

4. Comparison of LSE to theory

As in the case of fused silica, recent measurements of the ultrasonic attenuation of As_2S_3 have yielded results pertaining to the barrier heights of the defect states.[31] Therefore both the spectral distribution and the temperature dependence of the LSE can be compared to the predictions of the TJ model. In Sec. III B 3 the temperature dependence of the low-frequency Raman spectra of As_2S_3 has been presented. It is however more difficult to obtain the spectral distribution of the LSE. But by comparing low-temperature and higher-temperature spectra, the shape of the LSE can be determined.

Since the low-temperature (i.e., $T \approx 10$ K) Raman spectra is unencumbered by the presence of the LSE, the spectral features of the low-temperature low-frequency spectra can be wholly attributed to long-wavelength acoustic modes. The temperature dependence of the scattering arising from the acoustic modes is known to be proportional to $[n(\omega)+1]$.[19] Therefore by multiplying the intensity of the low-temperature spectra by $[n(\omega)+1]$, the resultant exhibits the spectral features that are attributed to the acoustic modes, but the contribution due to the LSE is absent. The low-temperature spectra modified by $[n(\omega)+1]$ can then be normalized to the higher-temperature spectra at a frequency outside the range of the LSE. The difference of the spectral intensities yields the LSE. This procedure has been carried out for the As_2S_3 glass and the resultant LSE spectral distribution is displayed as a dashed line in Fig. 12. The signal-to-noise ratio of the low-temperature spectra of $GeSe_2$ and GeS_2 was not adequate to justify a similar analysis for these glasses. Because the TJ model describes the spectral distribution of the LSE in the $I_{\perp\perp}/\omega[n(\omega)+1]$ spectrum, we also determine the contribution attributed to the LSE. This is accomplished by subtracting normalized low- and higher-temperature spectra. The contribution of the LSE to the $I_{\perp\perp}/\omega\,[n(\omega)+1]$ spectra for As_2S_3 is shown in Fig. 18(b).

In order to compare the predictions of the TJ model to the experimentally determined temperature dependence and spectral distribution of the LSE, the parameters V_m, V_0, and τ_0 of Eqs. (18) and (19) must be known. From analysis of the ultrasonic attenuation in As_2S_3 Ng and Sladek[31] (NS) have suggested several possible distributions of barrier heights. From the low-temperature attenuation NS have also suggested that the distribution of tunneling parameters is

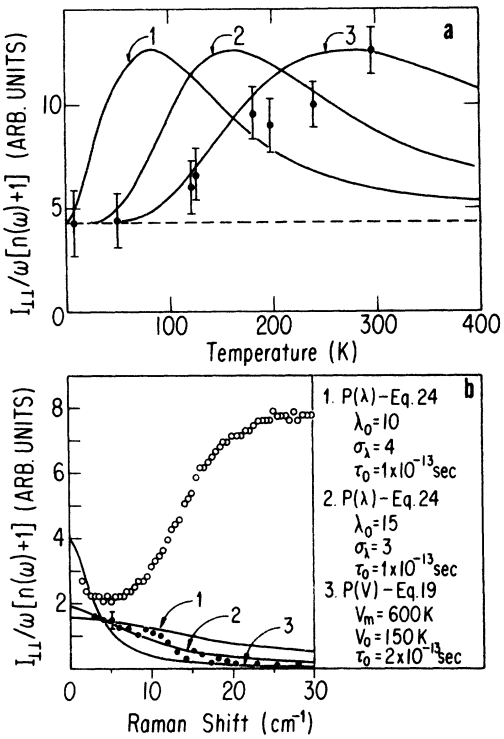

FIG. 18. (a) Temperature dependence of the As_2S_3 spectra at $\omega = 5$ cm^{-1}; and (b) the spectral distribution of the light-scattering excess. The solid circles in (b) represent the experimental spectral contribution due to the light-scattering excess while the open circles are the $I_{\perp\perp}/\omega[n(\omega)+1]$ data. The three different solid lines in (a) and (b) are plots of Eq. (18) with the values of the parameters indicated in (b). The dashed line in (a) is the contribution due to scattering from Debye phonons.

$$P(\lambda) = P(\lambda)\alpha \exp\left[-(\lambda-\lambda_0)^2/\sigma_\lambda^2\right] , \tag{24}$$

where λ_0 and σ_λ are dimensionless constants. The tunneling parameter λ is

$$\lambda \approx \tfrac{1}{2} d(2mV/\hbar^2)^{1/2} , \tag{25}$$

where m is the mass of the tunneling atom (or group of atoms) and d is the displacement between minima of the two well potential. Therefore if m and d are approximately constant for all defects

$$\int_{\lambda_{\min}}^{\lambda_{\max}} P(\lambda)\frac{\omega^2\tau}{1+\omega^2\tau^2}\,d\lambda \approx \int P(V)\frac{\omega^2\tau}{1+\omega^2\tau^2}\,dV , \tag{26}$$

where on the left-hand side $\tau = \tau_0 \exp(2\lambda^2\hbar^2/md^2)$. NS have found for $\tau_0 = 1\times10^{-13}$ sec that $\lambda_0 = 10$. The values of $\lambda_{\min}$ and $\lambda_{\max}$ used were 3 and 12. In addition they suggested the process involved an S atom tunneling over a distance of about 1 Å. Therefore from Eq. (25) the mean barrier height for this tunneling process is ~302 K. Using the left-hand side of Eq. (26) for the integral in Eq. (18) and the values of λ_0, $\lambda_{\max}$, $\lambda_{\min}$, τ_0, m, and

d indicated above, the theoretical spectral distribution at $T = 296$ and the temperature dependence of the LSE of As_2S_3 have been calculated. The results are compared to the experimental values in Figs. 18(a) and 18(b). The theoretical spectral function is normalized to the experimental data at 4 cm^{-1}, and the theoretical temperature dependence is scaled to give a maximum intensity equal to the experimental LSE intensity at $T = 296$. In addition, the theoretical temperature dependence has, as a baseline, the acoustic scattering contribution. As is evident from Fig. 18, neither the spectral dependence nor the temperature dependence are described well by the theoretical curves. However with $\tau_0 = 2\times10^{-13}$ sec a good fit to the spectral distribution was obtained, but the temperature dependence still deviated from the observed values.

From examination of the ultrasonic attenuation of As_2S_3 in the range $T = 100$–300 K, NS have obtained other values of the parameters λ_0, σ_λ, τ_0, and d of 15, 3, 1×10^{-13} sec, and 0.25 Å, respectively. And by assuming a barrier height V of ~475 K NS find that $m \approx 1.23\times10^{-21}$ g. We have used these values to ascertain the spectral and temperature dependence of the LSE as described above except that the integration over λ extended from $\lambda = 0$ to $\lambda = 30$. The results normalized as previously are displayed in Fig. 18. Here a good fit to the spectral distribution was obtained, but the theoretical temperature dependence deviates strongly from the observed results. The same ultrasonic attenuation data was analyzed by NS using a distribution of V instead of λ. They found agreement with the experimental attenuation using $P(V) = (V^3/6V_0^4)e^{-V/V_0}$, where $V_0 \approx 9300$ K. Examination of this function shows the maximum of $P(V)$ is at $V = 3V_0 \approx 27\,900$ K. Clearly relaxation of a defect with this magnitude of a barrier is unlikely at temperatures below 300 K.

We have varied the parameters V_0, V_m, and τ_0 of Eqs. (18) and (19) in an attempt to fit both the spectral and temperature dependence of the LSE of As_2S_3. The values examined ranged from $\tau_0 = 1\times10^{-14}$ to 1×10^{-12} sec, $V_m = 200$ to 700 K, and $V_0 = \frac{1}{5}V_m$ to $\frac{4}{5}V_m$. We were not able to satisfactorily describe both the spectral and temperature dependence of the LSE of As_2S_3. But with $\tau_0 = 2\times10^{-13}$ sec, $V_m = 600$ K, and $V_0 = 150$ K a somewhat reasonable agreement to the temperature dependence was obtained. The experimental curves obtained using the above values are also displayed in Fig. 18.

While the interpretation of the ultrasonic attenuation measurements does not yield conclusive values of V_0, V_m, and τ_0 for As_2S_3, it appears that the TJ model cannot describe both the spectral and temperature dependence of the LSE in As_2S_3. It is possible that a distribution of either τ_0 or $\Delta\alpha$ or both may be necessary to describe the spectral and temperature dependence of the LSE of As_2S_3 in terms of thermally activated relaxation of two-state defects.

5. *Composition dependence of LSE in alloys*

In this section the magnitude of the LSE for several compositions of the alloy system $(As_2S_3)_{1-x}(GeS_2)_x$ is presented. The low-frequency $\perp\perp$ Raman and $I_{\perp\perp}/\omega[n(\omega)+1]$ spectra of the alloy system $(As_2S_3)_{1-x}(GeS_2)_x$ is shown in Fig. 11. It is clear from Fig. 11 that the ratio of the magnitude of the LSE to that of the scattering at the frequency of the "boson peak" is greatest for As_2S_3 and smallest for GeS_2. In order to address the data in terms of the concentration of the local structural units we rewrite the alloy formula as $(AsS_{3/2})_{1-z}(GeS_2)_z$. In this formulation the ratio of the number of GeS_4 tetrahedral units to the number of AsS_3 pyramidal units is given by $z/(1-z)$. The parameter z is related to x by $z = x/(2-x)$.

The magnitude of the scattering at 4 cm^{-1} for the alloy system is shown in Fig. 19. The dashed line indicates the contribution due to scattering from long-wavelength acoustic modes. As is evidenced in Fig. 19, the magnitude of the LSE varies approximately linearly with z. The linear dependence of the LSE with z indicates that the probability of a structural two-state defect is greater for AsS_3

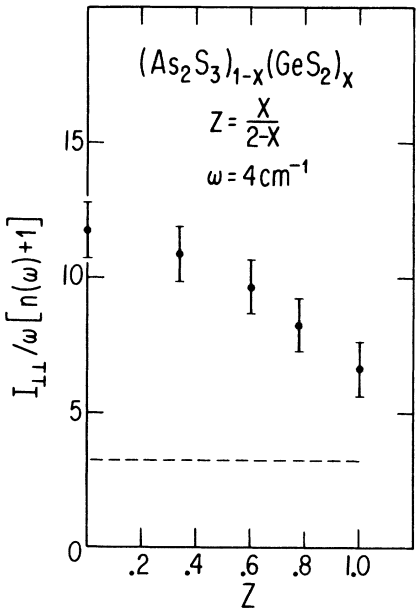

FIG. 19. Concentration dependence of the Raman intensity at 4 cm^{-1} of members of the alloy system $(As_2S_3)_{1-x}(GeS_2)_x$. The dashed line represents the contribution due to scattering from Debye phonons.

units than for GeS_4 units. This conclusion is supported by the fact that the four-way interconnected tetrahedral units will be less free to reorientate than the three-way interconnected pyramidal units.

However in the previous low-frequency light-scattering investigation of fused silica, it was noted that the magnitude of the LSE was dependent on the sample purity. Specifically fused silica with a higher content of OH impurities exhibited a LSE of greater magnitude than similar fused silica with a lower impurity concentration.[8] Therefore it is possible that differences in sample purity cause the linear concentration dependence of the LSE of the alloy system studied here. For the sample As_2S_3, both specific heat and ultrasonic attenuation measurements indicate that the concentration of two-level defects is of the order of 10^{17} cm^{-3}. Therefore even though high-purity (99.999%) powders were used for sample preparation, impurity effects cannot be ruled out. While slight deviations from stoichiometry could produce a large number of defects, the linear dependence of the magnitude of the LSE on concentration seems to preclude this possibility since a more complex functional dependence on z would be expected.

IV. SUMMARY AND CONCLUSIONS

An extensive investigation of the low-frequency light scattering from chalcogenide glasses has been described. Both wave-vector conserving Brillouin peaks and wave-vector nonconserving continuous scattering have been observed. The wave-vector nonconserving scattering in the low-frequency region arises from long-wavelength acoustic modes. The spectral distribution of the disorder-induced (wave-vector nonconserving) scattering is shown to agree with the prediction of a model by Martin and Brenig. By fitting the theoretical spectral form of the MB model to the low-frequency Raman spectra, a structural correlation range can be obtained. We found an SCR of ~6.5 Å for As_2S_3 and As_2Se_3 and an SCR of ~ 8.5 Å for GeS_2 and $GeSe_2$. Recent Raman measurements of GeS_2 and $GeSe_2$ which indicate ringlike structures of ~ 7.5 Å diameter support the SCR values obtained from the low-frequency scattering from acoustic modes. While the MB model described the spectral distribution of the low-frequency spectra successfully, the theoretical depolarization spectra deviated markedly from the experimentally determined spectra of the chalcogenide glasses. The failure of the MB model to describe the depolarization spectra of low-frequency Raman spectra appears to be the largest deficiency of the model. In the development of the MB model several assumptions and approximations were presented. Closer examination of these may yield the reason for the failure of the model to describe the depolarization spectra of the chalcogenide glasses.

After ascertaining the spectral contribution due to the long-wavelength acoustic modes, the light-scattering excess can be studied more quantitatively. The LSE was observed in the glasses As_2S_3, GeS_2, $GeSe_2$, and the alloys of the $(As_2S_3)_{1-x}(GeS_2)_x$ system. The temperature dependence of the LSE was found to be different from that which would be expected for scattering from boson excitations. In addition the observed temperature dependence ruled out the possibility that the LSE was due to two phonon summation or differences processes. The spectral distribution of the LSE of the As_2S_3 glass was also determined. It was found that the spectral distribution exhibited a half width at half maximum of ~11 cm^{-1}.

The spectral distribution and the temperature dependence of the LSE of As_2S_3 was compared with predictions of a recent theory of Theodorakopoulos and Jäckle. Using distributions of two-level defect states obtained from ultrasonic attenuation measurements of As_2S_3 the spectral and temperature dependence of the LSE was fit using the TJ model. While a reasonable agreement was obtained for the spectral form of the LSE the temperature dependence could not be fit. Additionally, when parameters were varied to fit the temperature dependence, the spectral distribution could not be described. Possibly by including in the model a distribution of polarizability differences of the defects and/or a distribution of relaxation lifetimes, the experimentally observed spectral distribution and temperature dependence of the LSE's of the chalcogenide glasses could be described. The TJ model also predicted an increase in the LSE at low temperatures due to quantum-mechanical tunneling. This increase was not observed. We suggest that the states which exhibit quantum-mechanical tunneling have a smaller polarizability difference than states which can only relax via thermal activation.

The magnitude of the LSE was found to display a linear decreasing dependence with respect to z for the alloy system $(AsS_{3/2})_{1-z}(GeS_2)_z$. We suggest that this may be due to the fact that three-way interconnected AsS_3 pyramidal units can reorientate more easily than four-way interconnected GeS_4 tetrahedral units. However impurity effects can not be completely ruled out as a possible cause.

ACKNOWLEDGMENTS

I especially wish to thank Professor S. A. Solin for his constant encouragement and guidance throughout this project. His valuable suggestions and helpful discussions are sincerely appreciated. Thanks are due to Dr. G. Lucovsky for giving us the high-quality samples necessary for this investigation. I also wish to thank M. Gorman for helpful discussions and E. J. Flynn for his assistance in obtaining the instrument transfer function.

---

*Research supported by the US ERDA. It has also benefitted from the general support of the University of Chicago Materials Research Laboratory by the NSF.

†Submitted in partial fulfillment of the requirements for the Ph.D. degree at the University of Chicago. Present address: Xerox Palo Alto Research Center, Palo Alto, Calif. 94304.

[1]M. H. Brodsky, in *Topics in Applied Physics*, edited by M. Cardona (Springer, Heidelberg, 1975), Vol. 8.

[2]A. J. Martin and W. Brenig, Phys. Status Solidi B 64, 163 (1974).

[3]W. Prettl, N. J. Shevchik, and M. Cardona, Phys. Status Solidi B 59, 241 (1973).

[4]J. S. Lannin, Solid State Commun. 12, 947 (1974).

[5]J. S. Lannin, Solid State Commun. 11, 1523 (1972).

[6]G. N. Papatheodorou and S. A. Solin, Phys. Rev. B 13, 1741 (1976).

[7]M. Gorman and S. A. Solin, Solid State Commun. 18, 1401 (1976).

[8]G. Winterling, Phys. Rev. B 12, 2432 (1975).

[9]G. Winterling, in *Proceedings of the Third International Conference on Light Scattering in Solids*, edited by M. Balkanski, R. C. C. Leite, and S. P. S. Porto (Flammarion, Campinas, 1975), p. 663.

[10]P. W. Anderson, B. I. Halperin, and C. M. Varma, Philos. Mag. 25, 1 (1972).

[11]W. A. Phillips, J. Low Temp. Phys. 7, 351 (1972).

[12]R. C. Zeller and R. O. Pohl, Phys. Rev. B 4, 2029 (1971).

[13]R. B. Stephens, Phys. Rev. B 8, 2896 (1973).

[14]G. Lucovsky and R. M. Martin, J. Non-Cryst. Solids 8-10, 185 (1972).

[15]R. J. Kobliska and S. A. Solin, Phys. Rev. B 8, 756 (1973).

[16]G. Locovsky, R. J. Nemanich, S. A. Solin, and R. C. Keezer, Solid State Commun. 18, 1576 (1975).

[17]G. Lucovsky, F. L. Galeener, R. C. Keezer, R. H. Geils, and H. A. Six, Phys. Rev. B 10, 5134 (1974).

[18]R. Loudon, Adv. Phys. 13, 423 (1974).

[19]R. Shuker and R. W. Gammon, Phys. Rev. Lett. 25, 222 (1970).

[20]J. E. Smith, Jr., M. H. Brodsky, B. L. Crowder, M. I. Nathan, and A. Pinczuk, Phys. Rev. Lett. 26, 642 (1971).

[21]L. Rauber, V. Minkiewicz, and C. Pelizzari (unpublished).

[22]R. J. Nemanich, M. Gorman, and S. A. Solin, Solid State Commun. (to be published).

[23]S. M. Shapiro, R. W. Gammon, and H. Z. Cummins, Appl. Phys. Lett. 6, 171 (1965).

[24]E. Whalley and J. E. Bertie, J. Chem. Phys. 46, 1264 (1967).

[25]J. Jäckle, Z. Phys. 257, 212 (1972).

[26]J. Jäckle, L. Piche, W. Arnold, and S. Hunklinger, J. Non-Cryst. Solids 20, 365 (1976).

[27]N. Theodorakopoulos and J. Jäckle, Phys. Rev. B 6, 2637 (1976).

[28]J. P. de Neufville, in *Optical Properties of Solids-Recent Developments*, edited by B. O. Seraphin (North-Holland, Amsterdam, 1975).

[29]J. Cernogora, F. Mollet, C. Benoit à La Guillaume, and M. Jouanne, Solid State Commun. 19, 465 (1976).

[30]I. L. Fabelinskii, *Molecular Scattering of Light* (Plenum, New York, 1968), p. 152.

[31]D. Ng and R. J. Sladek, Phys. Rev. B 11, 4017 (1975).

[32]N. Soga, M. Kunugi, and R. Ota, J. Phys. Chem. Solids 34, 2143 (1973).

[33]P. Flubacher, A. J. Leadbetter, J. A. Morrison, and B. P. Stoicheff, J. Phys. Chem. Solids 12, 53 (1959).

[34]R. K. Galkiewicz and J. Tauc, Solid State Commun. 10, 1261 (1972).

[35]S. A. Solin, in *Proceedngs of the International Conference on Structure and Excitations of Amorphous Solids*, edited by G. Lucovsky and F. L. Galeener (AIP, Williamsburg, 1976), p. 205.

[36]J. P. de Neufville, S. C. Moss, and S. R. Ovshinsky, J. Non-Cryst. Solids 13, 191 (1973/74).

[37]H. R. Klug and L. E. Alexander, *X-Ray Diffraction Procedures* (Wiley, New York, 1974), p. 687.

[38]S. C. Rowland, S. Narasimhan, and A. Bienenstock, J. Appl. Phys. 43, 2741 (1972).

[39]R. W. Fawcett, C. N. J. Wagner, and G. S. Cargill, III, J. Non-Cryst. Solids 8-10, 369 (1972).

[40]G. S. Cargill, III (private communication).

[41]R. J. Nemanich, S. A. Solin, and G. Lucovsky, Solid State Commun. (to be published).

[42]N. Morimoto, Mineral. J. (Sapporo) 1, 160 (1954).

[43]R. J. Nemanich, S. A. Solin, and G. Lucovsky, in *Proceedings of the Sixth International Conference on Amorphous and Liquid Semiconductors*, edited by B. T. Kolomiets (Nauka, Leningrad, 1975), p. 518.